Received: 5 July 2024 | Revised: 17 September 2024 | Accepted: 18 September 2024

DOI: 10.1002/alz.14329

Alzheimer's & Dementia®
THE JOURNAL OF THE ALZHEIMER'S ASSOCIATION

RESEARCH ARTICLE

Thorase deficiency causes both Aβ accumulation and tau hyperphosphorylation in mouse brain

Han Zhang[1] | Menghua Cai[1] | Fei Gao[1] | Jia Yang[1] | Chao Li[1] | Jingyi Han[1,2] | Yue Wang[1] | Yi Xu[1] | Yu Hu[1] | Hui Chen[1] | Wei He[1] | Jianmin Zhang[1,3]

[1]Department of Immunology, CAMS Key laboratory T cell and Cancer Immunotherapy, Institute of Basic Medical Sciences, Chinese Academy of Medical Sciences and School of Basic Medicine, Peking Union Medical College, State Key Laboratory of Common Mechanism Research for Major Diseases, Beijing, China

[2]Department of Thoracic Surgery, Qilu Hospital of Shandong University, Jinan, Shandong, China

[3]Changzhou Xitaihu Institute for Frontier Technology of Cell Therapy, Changzhou, Jiangsu Province, China

Correspondence
Hui Chen, Jianmin Zhang, and Wei He, Department of Immunology, CAMS Key laboratory T cell and Cancer Immunotherapy, Institute of Basic Medical Sciences, Chinese Academy of Medical Sciences and School of Basic Medicine, Peking Union Medical College, State Key Laboratory of Common Mechanism Research for Major Diseases, Beijing, 100005, China.
Email: chenhui@ibms.pumc.edu.cn, jzhang42@163.com and heweingd@126.com

Funding information
National Key Research and Development Program of China, Grant/Award Number: 2022YFC3602004; CAMS Initiative for Innovative Medicine, Grant/Award Numbers: 2021-I2M-1-005, 2021-I2M-1-035, 2021-I2M-1-053; National Natural Science Foundation of China, Grant/Award Numbers: U20A20374, 32270915, 82071791; Institute of Basic Medical Sciences; Chinese Academy of Medical Sciences; Neuroscience Center; China Human Brain Banking Consortium

Abstract

INTRODUCTION: The pathogenesis of two major pathogenic characters—amyloid beta (Aβ) accumulation and hyperphosphorylated tau protein—in the brains of patients with Alzheimer's disease (AD) remains unclear.

METHODS: Western blot and immunofluorescence staining were performed to detect the proteins in the brains of Thorase conditional knockout/transgenic mice and their littermates. A co-immunoprecipitation assay was applied to examine the Thorase-interacting proteins.

RESULTS: Genetic deletion of Thorase resulted in tau hyperphosphorylation and promoted Aβ accumulation in the mouse brain. Conversely, Thorase overexpression alleviated the pathogenesis of AD. Thorase regulated the phosphorylation of tau by targeting specific kinases and theprotein phosphatase 2B (PP2B). Thorase deficiency also impaired microglial phagocytosis and induced neuroinflammation by the activation of the NOD-like receptor thermal protein domain associated protein 3 (NLRP3) inflammasomes in microglia.

DISCUSSION: Thorase may be a potential druggable target for developing therapeutic approaches to treat AD and other neurodegenerative diseases.

KEYWORDS
Alzheimer's disease, Aβ, microglia, PP2B, tau protein, Thorase

Highlights

- Thorase deletion leads to elevated amyloid beta (Aβ) deposition and hyperphosphorylated tau accumulation in the brain.
- Thorase regulates the phosphorylation of tau protein via PP2B.
- Thorase deficiency impairs microglial phagocytosis and promotesNLRP3-mediated neuroinflammation.

Han Zhang, Menghua Cai, Fei Gao, Jia Yang, and Chao Li contributed equally to this study.

- Overexpression of Thorase alleviates Aβ deposition and tau phosphorylation in the AD mouse model.

1 | BACKGROUND

Alzheimer's disease (AD) is a progressive neurodegenerative disorder characterized by the primary manifestations of cognitive impairment and progressive memory loss and is accompanied by a reduced ability to learn, work, and perform daily activities.[1] AD is pathologically defined by histopathological lesions such as extracellular amyloid beta (Aβ) plaque deposition and intraneuronal neurofibrillary tangles (NFTs), which result from the accumulation of hyperphosphorylated tau protein, as well as other pathological events, including elevated activated microglia and impaired mitochondrial respiration.[2] Aβ is generated by the cleavage of amyloid precursor protein (APP) by proteolytic secretase, and Aβ monomers can aggregate into Aβ oligomers, fibrils, and eventually amyloid plaques, which impair immune responses in microglia and trigger neuronal damage.[3] Aβ has been widely accepted as an initiating event that leads to other pathological changes in AD.[4,5]

Encoded by the *MAPT* gene on chromosome 17, tau protein is a member of the microtubule-associated protein (MAP) family. The longest isoform of the tau protein has 85 potential phosphorylation sites.[6] A number of protein kinases, including glycogen synthase kinase 3β (GSK3β), mitogen activated protein kinase (MAPK), cyclin-dependent kinase 5 (CDK5)/p35, and protein kinase A (PKA), are involved in the phosphorylation of the tau protein, and several phosphatases, such as protein phosphatase 1 (PP1), protein phosphatase 2A (PP2A), PP2B, and protein phosphatase 5 (PP5), can drive the reversal and dephosphorylation of the tau protein.[7,8] In neurodegenerative disorders, the tau protein is hyperphosphorylated at key sites, predominantly at serine or threonine (Ser/Thr) residues, such as Ser202/Thr205, Ser212/Thr214, Thr231, Ser262, and Ser396/Ser404.[9,10] The hyperphosphorylation contributes to the loss of microtubule-binding ability, charge distribution, autoaggregation, and aberrant conformational modifications. Progressively abnormal levels of the phosphorylated tau protein result in the formation of soluble aggregates, which are toxic to microglia and neurons, and insoluble deposits, including paired helical filaments (PHFs) and NFTs. Increasing evidence suggests that these soluble hyperphosphorylated tau aggregates and PHFs are neurotoxic to neurons, leading to neurodegeneration during the pathological process of AD.[11]

Neuroinflammation also plays a vital role in the pathogenesis of AD through the secretion of neurotoxic products and proinflammatory cytokines by activated microglia and astrocytes, which results in neuronal dysfunction and cell death.[12] NLRP3 has been implicated in AD and induces the cleavage of cytokine precursors, leading to neuroinflammation through active interleukin-1β (IL-1β) and interleukin-18 (IL-18).[13] Recent studies have shown that NLRP3 inflammasome activation enhances Aβ plaque deposition by reducing Aβ phagocytosis and promotes tau hyperphosphorylation to tangle formation in AD, suggesting that NLRP3 inflammasome activation plays a crucial role in the pathological development of AD.[14,15]

The AAA^+ ATPase Thorase, also named ATPase family AAA domain containing 1 (ATAD1), is located at the mitochondrial outer membrane and maintains mitochondrial quality control and regulates α-amino-3-hydroxy-5-methyl-4-isoxazole propionic acid (AMPA) receptor–dependent synaptic plasticity.[16–18] Our previous studies found that 80% of Thorase knockout (KO) mice have a lifespan of only 19 to 25 days after birth, and the overexpression of Thorase provides neuroprotective effects that improve neuronal survival in response to glutamate excitotoxicity and ischemic injury in vivo.[19] It is important to note that previous studies identified ATAD1 as one of the AD-related blood-secretory proteins through a comparison analysis from three databases and one of the AD-associated genes in a comprehensive proteomic analysis.[20,21] Msp1, the ortholog of Thorase in yeast, has been proven to promote the degradation and removal of mislocalized tail-anchored (TA) proteins, as well as to maintain mitochondrial protein import capacity.[17,22]

Here, our results demonstrate that Thorase deficiency promotes Aβ plaque deposition, hyperphosphorylated tau protein accumulation, and increased activated microglia, resulting in severe neuroinflammation and progression of AD. In contrast, overexpression of Thorase contributed to alleviating pathological symptoms in AD, indicating that Thorase may serve as a novel therapeutic target for AD treatment.

2 | METHODS

2.1 | Antibodies, reagents, and plasmids

The antibodies used in this study are described in Table S1.

The following reagents were used in this study: protease inhibitors and protease and phosphatase inhibitors (Thermo Fisher Scientific, Waltham, MA, USA), jetPRIME Transfection Reagent (Polyplus Transfection, Illkirch, France), Prolong Gold Antifade Mountant (Thermo Fisher Scientific, Waltham, MA, USA), SuperSignal West Pico PLUS Chemiluminescent Substrate (Thermo Fisher Scientific, Waltham, MA, USA), bicinchoninic acid assay (BCA) kit (Thermo Fisher Scientific, Waltham, MA, USA), 3, 3'-diaminobenzidine (DAB) kit (ZSGB, Beijing, China), and horseradish peroxidase (HRP) anti-rabbit/mouse kit (Vector Laboratories, Newark, CA, USA).

The PP2B Aα plasmid and the PP2B Aβ plasmid were purchased from Addgene. The cFUGW-GFP plasmid was a gift from Shiyou Li at the Beijing Institute of Genome Research, Chinese

Academy of Sciences. cFUGW-PP2B Aα-GFP, cFUGW-PP2B Aβ-GFP, cFUGW-Thorase-Myc, and cFUGW-Tau WT-GFP were constructed from cFUGW-GFP.

2.2 | Ethics and human sample

All brain tissues from non-AD and AD patients were obtained from the National Developmental and Functional Human Brain Bank Chinese Academy of Medical Sciences (CAMS) and Peking Union Medical College (PUMC), Beijing, China. All donors provided informed consent for using their donated body tissues for medical research. Detailed information on donors is described in Table S2.

2.3 | Mouse handling

All mouse breeding and handling procedures were approved by the Institutional Animal Care and Use Committee (IACUC) of CAMS and PUMC. Thorase$^{+/-}$ mice, Thorase$^{flox/+}$ mice, and conditional Thorase transgenic (cTg) mice were donated by Drs. Ted Dawson and Valina Dawson from the Institute of Cell Engineering, Johns Hopkins University School of Medicine. The CaMKIIa-iCre mice were obtained originally from the European Mouse Mutant Archive (EMMA ID: EM01153)[23] and crossed with Thorase$^{flox/+}$ mice for generating conditional Thorase knockout (cKO) mice. B6;C3-Tg(APPswe, PSEN1dE9)85Dbo/Mmjax (referred to as APP/PS1) transgenic mice were obtained from the Jackson Laboratory (Bar Harbor, ME, USA). Thorase cKO-APP/PS1 mice and Thorase cTg-APP/PS1 mice were generated by two rounds of crossing Thorase cKO mice and Thorase cTg mice, respectively, with APP/PS1 transgenic mice. Detailed information on the mice used in this study is shown in Figure S1.

2.4 | Mouse genotyping

The genotypes of the mice were determined via polymerase chain reaction (PCR) of DNA obtained from tail screening.[24] The primers used for genotyping Thorase$^{-/-}$ and Thorase$^{flox/+}$ mice were JZ129, JZ156, and JZ178. The primers used for genotyping CaMKIIa-iCre mice were JZ179 and JZ180. The primers used for genotyping Thorase cTg mice were JZ258, JZ259, JZ262, and JZ263. The primers used for APP/PS1 mice genotyping were OMIR3610, OMIR3611, OMIR7338, and OMIR7339. The sequences of primers are listed in Table S3.

2.5 | Isolation and treatment of primary microglia

Primary microglial cultures were prepared from early postnatal (P0–P1) mouse brains and isolated as described previously.[25] Microglia were cultured in DMEM/F-12 medium (Thermo Fisher Scientific, Waltham, MA, USA) supplemented with 10% fetal bovine serum (FBS) (Thermo Fisher Scientific) at 37°C and 5% CO_2. Half of the medium was changed every 3–4 days, and the mixed cultured glial cells were observed to spread all over the bottom of the plate for ≈10–14 days. Microglia were collected by gentle trypsin digestion (Thermo Fisher) and plated in 24-well plates for immunostaining and phagocytosis assays. After 12 h of culture, we added LPS, ATP, and Aβ peptides to the microglia for 3 or 24 h. Then we collected the supernatant and cells for the next experiment.

RESEARCH IN CONTEXT

1. **Systematic review**: The authors reviewed the literature using PubMed. Alzheimer's disease (AD) is a progressive neurodegenerative disorder characterized by two major pathogenic lesions: amyloid beta (Aβ) deposition and tau protein hyperphosphorylation.
2. **Interpretation**: Our results demonstrate that genetic deletion of Thorase resulted in tau hyperphosphorylation and enhanced Aβ accumulation in the mouse brain. In contrast, overexpression of Thorase contributed to alleviating pathological symptoms in AD.
3. **Future directions**: Our findings elucidate a novel insight into the pathogenesis of AD, and Thorase may be a potential druggable target for developing therapeutic approaches to treat AD and other neurodegenerative diseases.

2.6 | Western blot analysis

We lysed mouse brain tissues with RIPA buffer containing protease and phosphatase inhibitors (Thermo Fisher Scientific) and centrifuged them at 12,000 × *g* for 15 min at 4°C. The supernatant was collected for immunoblot analysis, and protein concentrations were determined using a BCA assay kit (Thermo Fisher Scientific). Approximately 15–20 μg of protein was separated via SDS–PAGE, after which the proteins were transferred to NC membranes. After the membranes were blocked with 5% bovine serum albumin (BSA) in TBST buffer for 2 h, the primary antibody was added to the NC membranes and incubated overnight at 4°C. Then we washed the membranes with TBST buffer three times and added HRP-labeled goat anti-rabbit/mouse secondary antibodies for 1 h. SuperSignal West Pico PLUS Chemiluminescent Substrate (Thermo Fisher Scientific) was used to detect horseradish peroxidase (HRP) on the NC membranes using ChemiScope (CLiNx Science Instruments, Shanghai, China). We measured the gray values of the bands and statistically analyzed the relative expression levels of the target proteins using ImageJ software and GraphPad Prism version 8 software.

2.7 | Immunohistochemistry staining

The mice were transcardially perfused with phosphate-buffered saline (PBS) for 5 min and ice-cold 4% paraformaldehyde (PFA) for 30 min as

described previously.[26] For paraffin slices, the brain tissues were sectioned into 4 μm for 10 slices and stored at room temperature. The slides were dewaxed in dimethylbenzene for 10 min twice and placed in 100%, 95%, 90%, and 80% alcohol for 5 min. After antigen repair and endogenous peroxidase removal, the slides were incubated with normal goat serum for 30 min to block nonspecific sites. We diluted the primary antibodies with goat serum and incubated the antibodies with the sections for 1.5 h in a dark, humid chamber. For immunohistochemistry, after incubation with ImmPRESS Polymer Reagent Peroxidase secondary antibody solution at room temperature for 1 h, the slices were stained with DAB buffer and hematoxylin counterstaining. Finally, the slices were dehydrated before being cover-slipped. We used a Leica DM6 B microscope to scan the slices.

2.8 | Immunofluorescence staining

All procedures were performed following the manufacturer's instructions.[27] The mice brain tissues were paraffin embedded and sectioned into 4 μm for 8–10 slices. For tissue immunofluorescence staining, after the primary antibodies were added, we used Alexa Fluor 488-labeled and 555-labeled anti-mouse/rabbit fluorescent secondary antibodies (CST) to stain the slices. Then the sections were covered with ProLong Gold Antifade Mountant (Thermo Fisher Scientific) after staining with DAPI (Thermo Fisher Scientific). We observed the cells using a Zeiss LSM780 confocal microscope and analyzed the results with Zeiss ZEN Service Blue software.

2.9 | Thioflavin-S staining

Thioflavin-S dye solution was freshly prepared and kept away from light as described in the manufacturer's instructions.[28] The brain tissue slides were permeabilized in PBS containing 0.25% Triton X-100 and incubated at a low speed for 20 min. Then the slices were stained with thioflavin-S dye solution and incubated at room temperature in a wet box away from light for 10 min. After staining, the slices were placed in 50%, 80%, and 95% gradient alcohol for decolorization for 10 min each time. Next the slices were incubated with DAPI at room temperature for nuclear staining. We covered the sections with ProLong Gold Antifade Mountant (Thermo Fisher Scientific) and dried them at room temperature for subsequent confocal microscopy observation.

2.10 | Co-immunoprecipitation assay

We cotransfected 293T cells with the plasmids cFUGW-Thorase-myc, cFUGW-PP2B Aα-GFP, cFUGW-PP2B Aβ-GFP, or cFUGW-GFP using jetPRIME Transfection Reagent (Polyplus Transfection, Illkirch, France) according to the manufacturer's instructions.[29] After 48 h of transfection, the cells were washed twice with PBS and collected in lysis buffer containing 25 mM Tris base, 150 mM NaCl, 1 mM EDTA, 0.5% NP-40, 1% Triton X-100, 0.5% deoxycholate, and protease and phosphatase inhibitors (Thermo Fisher Scientific) on ice. The supernatants were precleared with 10 μL of uncoupled agarose beads after centrifugation, and the protein concentration was determined by using a BCA assay kit (Thermo Fisher Scientific). Precleared immunocomplexes were incubated with GFP-Trap or Myc-Trap beads (ChromoTek, Munich, Germany) for 12–16 h and collected for the IP samples. Western blotting was subsequently performed to examine the interaction between Thorase and both PP2B Aα and PP2B Aβ using anti-GFP and anti-Myc antibodies.

2.11 | Enzyme-linked immunosorbent assay (ELISA)

All procedures were performed following the manufacturer's instructions.[30] For measuring Aβ_{40} and Aβ42 peptide deposition in the brain and tumor necrosis factor α (TNFα), IL-6, and IL-1β cytokine levels, brain tissues were isolated from Thorase cKO-APP/PS1 mice (n = 3) and their APP/PS1 littermates or Thorase cTg-APP/PS1 mice (n = 4) and their littermates. The brain tissues were lysed with RIPA lysis buffer (20 mM Tris-HCl, 150 mM NaCl, 1.0% NP-40, 1.0% sodium deoxycholate, and 0.1% SDS) supplemented with protease inhibitors (Thermo Fisher Scientific). The supernatants and cell lysates were collected for measurements of TNFα, IL-6, and IL-1β levels.

2.12 | Lactate dehydrogenase release assay

The cell supernatants were collected and added to the 96-well plates for 50 μL each well as described in the manufacturer's instructions.[31] The cell culture medium was used as blank control, and three biological replicates were set for each sample. We added 50 μL CytoTox 96 Reagent to each well and incubated at room temperature for 30 min. Then we added 50 μL Stop Solution to each well of the 96-well plate and used an enzymoscope to measure the OD value of the sample at 490 or 492 nm.

2.13 | Statistical analysis

The data were statistically analyzed using GraphPad Prism version 8 for Windows (GraphPad Software, La Jolla, CA, USA) and Microsoft Office Excel Software version 16.74. National Institutes of Health (NIH) ImageJ software was used for the quantification of the Western blotting and immunofluorescence staining data. For immunohistochemistry statistics, we collected 3–4 sections unbiased stereologically from each mouse brain by using a Leica DM6B microscope at 20× magnification with Stereo Investigator version 6.0 software (MicroBright-Field, MBF Bioscience, Williston, VT, USA) as described in our previous study.[32] Then we calculated the phosphorylated tau protein or amyloid plaque percentage covering the area in the cortex and hippocampus separately. The phosphorylated levels in the cortex and hippocampus were quantified using ImageJ software. The results were assessed for normality using the unpaired Student's t-test,

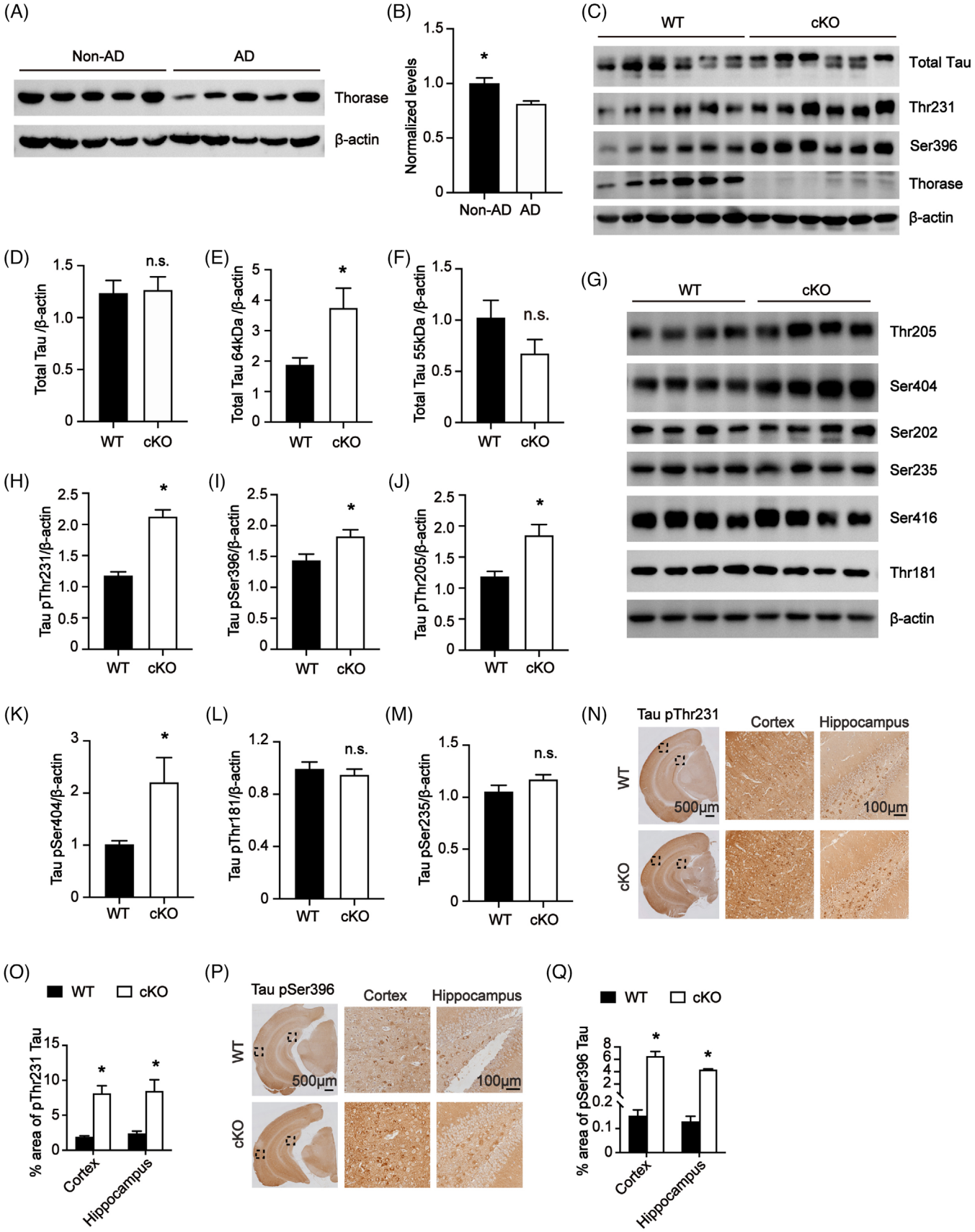

FIGURE 1 Thorase expression is reduced in the brains of patients with Alzheimer's disease (AD), and Thorase conditional knockout (cKO) mice exhibited an elevated level of hyperphosphorylated tau protein in the brains. (A) Western blot analysis of the expression levels of Thorase in the

and multigroup comparisons were performed using one-way analysis of variance (ANOVA) and unpaired two-tailed Student's *t*-tests. The data are expressed as the mean ± standard error of measurement (SEM). Significant differences are presented as n.s. (not significant), $^{*}p < 0.05$, $^{**}p < 0.01$, and $^{***}p < 0.001$.

3 | RESULTS

3.1 | Thorase expression is reduced in the brain tissues of patients with AD

Previous studies identified Thorase as one of the AD-associated genes in a comprehensive proteomic analysis.[21] Our previous studies have proven that Thorase deficiency in mice leads to AD-like neurodegenerative behaviors, such as deficits in short-term memory.[16] Thus we analyzed the expression level of Thorase in the brain tissues from patients with AD. Western blots showed a decrease of Thorase expression in brain tissues from five AD patients compared with tissue from five age-matched donors without any symptoms of AD (Figure 1A,B), indicating that Thorase may be involved in the pathogenesis of AD.

3.2 | Thorase cKO mice exhibited elevated level of hyperphosphorylated tau proteins in the brain

Then we examined the levels of phosphorylated tau proteins at various sites in the brain tissues of Thorase cKO mice and their wild-type (WT) littermates. Western blot analysis showed that although no significant change was observed in total tau protein expression between WT and cKO mice (Figure 1C,D), the levels of hyperphosphorylated tau proteins, which referred to 64 kDa bands, were elevated significantly in cKO mice compared with those in WT mice, whereas lower levels of non-phosphorylated tau protein, which referred to 55 kDa bands, were observed in cKO mice (Figure 1E,F). Then we examined the levels of phosphorylated tau proteins at different sites. The results showed that Thorase cKO mice exhibited elevated levels of hyperphosphorylated tau proteins at Thr231 (Figure 1C,H), Ser396 (Figure 1C,I), Thr205 (Figure 1G,J), and Ser404 sites (Figure 1G,K). There was no significant difference in the level of the phosphorylated tau proteins at Thr181 and Ser235 sites (Figure 1L,M). In addition, immunohistochemical staining revealed increased levels of the tau protein phosphorylated at the Thr231 and Ser396 sites in Thorase cKO mice (Figure 1N–Q), consistent with the Western blot findings. These results, taken together, reveal that Thorase regulates the phosphorylation of specific sites on tau proteins.

3.3 | Thorase overexpression reduces the levels of tau phosphorylation at specific Ser396, Thr231, and Ser404 sites

Next we examined the levels of tau phosphorylation in the brains of Thorase cTg mice and their WT littermates at the age of about 11 months. Western blot analysis showed no significant change in total tau protein in Thorase cTg mice (Figure 2A,B). The levels of phosphorylated tau proteins were decreased significantly at several specific sites, including Thr231 (Figure 2A,C), Ser396 (Figure 2A,D), and Ser404 (Figure 2A,E) sites, in the brains of Thorase cTg mice. However, no significant difference was observed in the level of the phosphorylated tau proteins at the Thr205 (Figure 2A,F), Ser235, and Thr181 sites (Figure 2A). In addition, immunohistochemical staining also revealed decreased levels of the tau protein phosphorylated at the Thr231 and Ser396 sites in the brains of Thorase cTg mice (Figure 2G–J), consistent with the Western blot findings.

3.4 | Thorase regulates the tau phosphorylation by targeting specific kinases or phosphatases

Tau protein contains abundant of phosphorylation sites that are regulated by several protein kinases, such as MAPK, GSK3β, and CDK5, and phosphatases such as PP2A, PP2B, and PP1. Given the changes of phosphorylation levels on different sites of tau proteins in the brains of Thorase cKO mice as shown in Figure 1, we examined the expression

brains of AD patients or non-AD donors. β-Actin was used as a protein loading control. (B) Quantification of the integral optical density (IOD) of Thorase normalized to β-actin ($n = 5$) in panel A. (C) Western blot analysis of phosphorylated tau protein levels at Thr231 and Ser396 sites from the brain tissue of Thorase cKO mice and their wild-type (WT) littermates at the age of 5 months ($n = 6$). (D) Quantification of the IOD of total tau protein normalized to β-actin in panel C. (E) Quantification of the IOD of 64 kDa total tau protein normalized to β-actin in panel C. (F) Quantification of the IOD of 55 kDa total tau protein normalized to β-actin in panel C. (G) Western blot analysis of phosphorylated tau protein levels at several sites in the brain tissue of Thorase cKO mice and WT littermates ($n = 4$). (H) Quantification of the IOD of phosphorylated tau protein at Thr231 site normalized to β-actin in panel C. (I) Quantification of the IOD of phosphorylated tau protein at Ser396 site normalized to β-actin in panel C. (J) Quantification of the IOD of phosphorylated tau protein at Thr205 site normalized to β-actin in panel G. (K) Quantification of the IOD of phosphorylated tau protein at Ser404 site normalized to β-actin in panel G. (L) Quantification of the IOD of phosphorylated tau protein at Thr181 site normalized to β-actin in panel G. (M) Quantification of the IOD of phosphorylated tau protein at Ser235 site normalized to β-actin in panel G. (N) Immunohistochemistry staining of phosphorylated tau protein at Thr231 sites in the cortex and hippocampus of 5-month-old Thorase cKO mice and WT littermates ($n = 4$). Scale bar, 500 mm (left) and 100 μm (right). (O) Quantification of the % area of phosphorylated tau protein at Thr231 site in the cortex and hippocampus in panel N. (P) Immunohistochemistry staining of phosphorylated tau protein at Ser396 sites in the cortex and hippocampus of 5-month-old Thorase cKO mice and WT littermates ($n = 3$). (Q) Quantification of the % area of phosphorylated tau protein at Ser396 site in the cortex and hippocampus in panel P. Data are presented as the mean ± standard error of measurement (SEM) determined using unpaired two-tailed Student's *t*-test. n.s., not significant; $^{*}p < 0.05$.

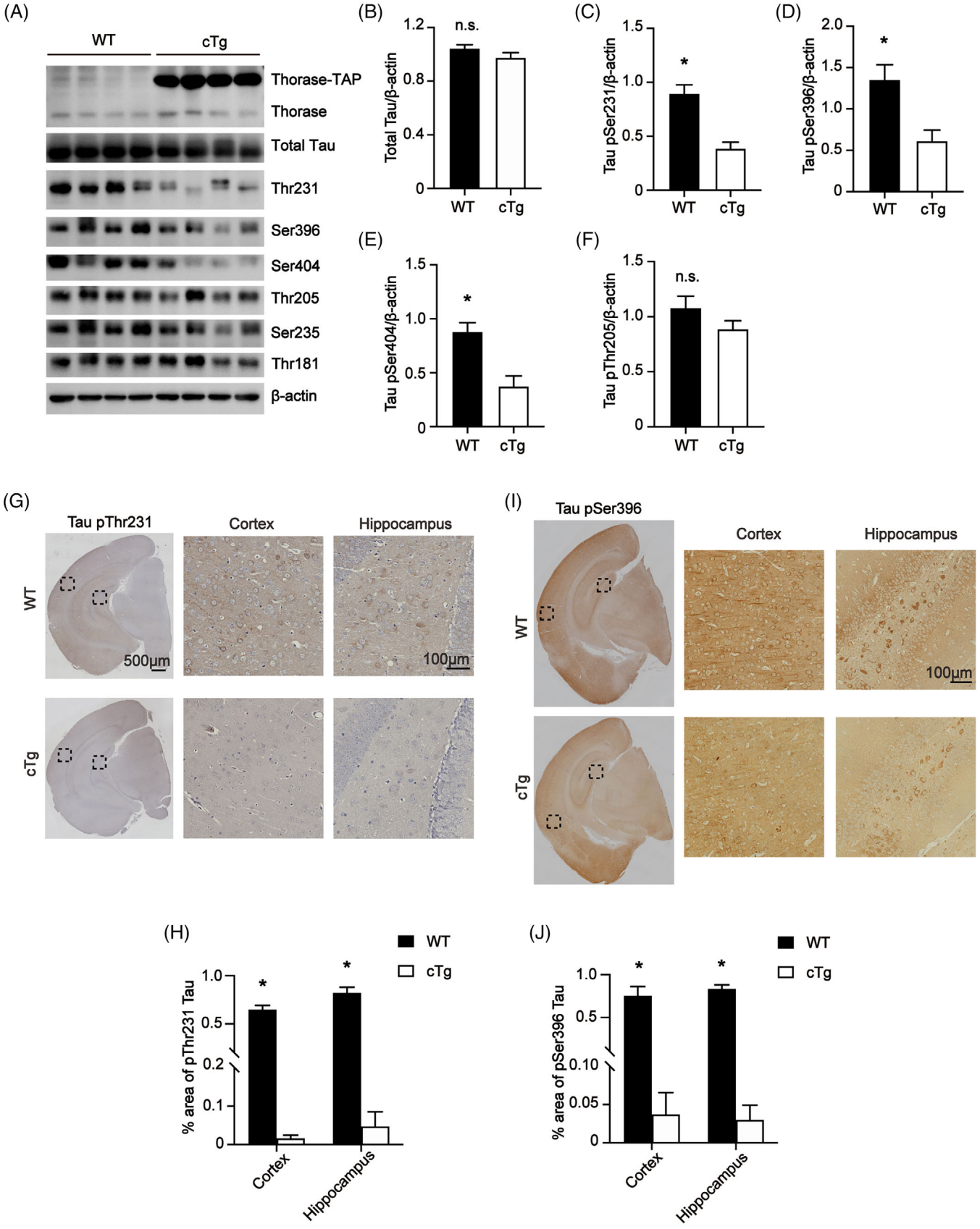

FIGURE 2 Thorase overexpression reduces the levels of tau phosphorylation at specific Ser396, Thr231, and Ser404 sites. (A) Western blot analysis of phosphorylated tau protein levels at several sites from the brain tissue of Thorase cTg mice and their wild-type (WT) littermates at the age of 11 months ($n = 4$). (B) Quantification of the integral optical density (IOD) of total tau protein normalized to β-actin in panel A. (C)

Quantification of the IOD of phosphorylated tau protein at Thr231 site normalized to β-actin in panel A. (D) Quantification of the IOD of phosphorylated tau protein at Ser396 site normalized to β-actin in panel A. (E) Quantification of the IOD of phosphorylated tau protein at Ser404 site normalized to β-actin in panel A. (F) Quantification of the IOD of phosphorylated tau protein at Thr205 site normalized to β-actin in panel A. (G) Immunohistochemistry staining of phosphorylated tau protein at Thr231 site in the cortex and hippocampus of 11-month-old Thorase cTg mice and WT littermates ($n = 3$). Scale bar, 500 mm (left) and 100 μm (right). (H) Quantification of the % area of phosphorylated tau protein at Thr231 site in the cortex and hippocampus in panel G. (I) Immunohistochemistry staining of phosphorylated tau protein at Ser396 site in the cortex and hippocampus of 11-month-old Thorase cTg mice and WT littermates ($n = 3$). (J) Quantification of the % area of phosphorylated tau protein at Ser396 site in the cortex and hippocampus in panel I. Data are presented as the mean ± standard error of measurement (SEM) determined using unpaired two-tailed Student's *t*-test. n.s., not significant; $^{*}p < 0.05$.

levels of specific site-corresponding protein kinases and phosphatases in the brains of Thorase cKO mice (Figure S2A). Although no significant difference was observed in the expression levels of the protein kinases GSK3β, P38 MAPK, Erk1/2 MAPK, or CDK5R1 P35 (Figure 3A and Figure S2B), the expression levels of phosphorylated p-GSK3β Y216, p-P38 MAPK T180/Y182, and p-Erk1/2 MAPK T202/Y204 decreased significantly (Figure 3A,B). As for the phosphatases, we found that the expression levels of the phosphatases PP2B Aα and PP2B Aβ isomers decreased in Thorase cKO mouse brain tissue, whereas the phosphatases PP2A A, PP2A C, PP1, and PP5 showed no significant

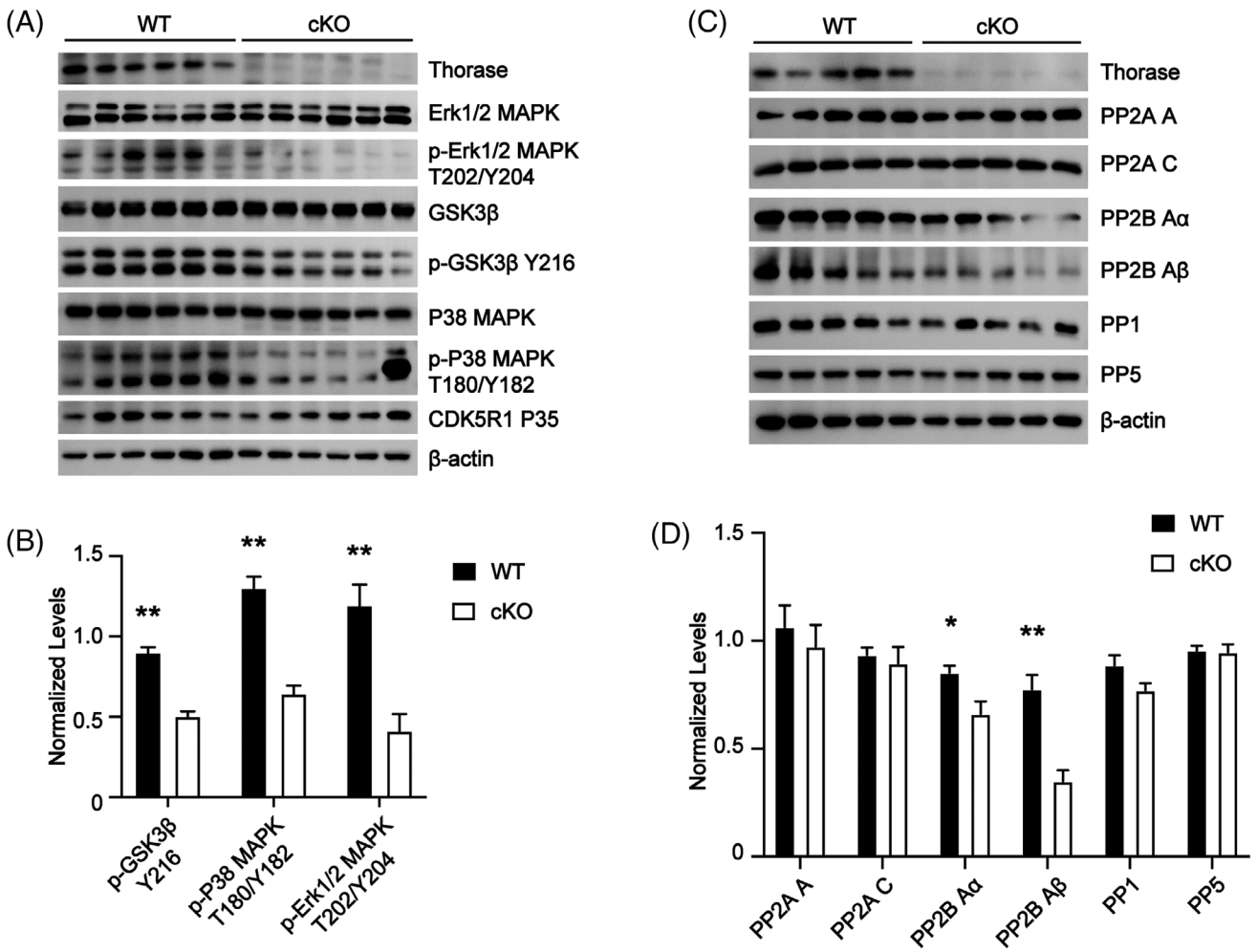

FIGURE 3 Thorase regulates the tau phosphorylation by targeting specific kinases or phosphatases. (A) Western blot analysis of phosphorylation levels of p-Erk1/2 MAPK T202/Y204, p-GSK3β Y216, and p-P38 MAPK T180/Y182 from the brain tissue of Thorase conditional knockout (cKO) mice and wild-type (WT) littermates at the age of 5 months ($n = 6$). (B) Quantification of the integral optical density (IOD) of phosphorylation levels of p-Erk1/2 MAPK T202/Y204, p-GSK3β Y216, and p-P38 MAPK T180/Y182 normalized to β-actin in panel A. (C) Western blot analysis of the expression levels of phosphatases from the brain tissue of Thorase cKO mice and WT littermates at the age of 5 months ($n = 5$). (D) Quantification of the IOD of the expression levels of phosphatases normalized to β-actin in panel C. Data are presented as the mean ± standard error of measurement (SEM) determined using unpaired two-tailed Student's *t*-test. n.s., not significant; $^{*}p < 0.05$ and $^{**}p < 0.01$.

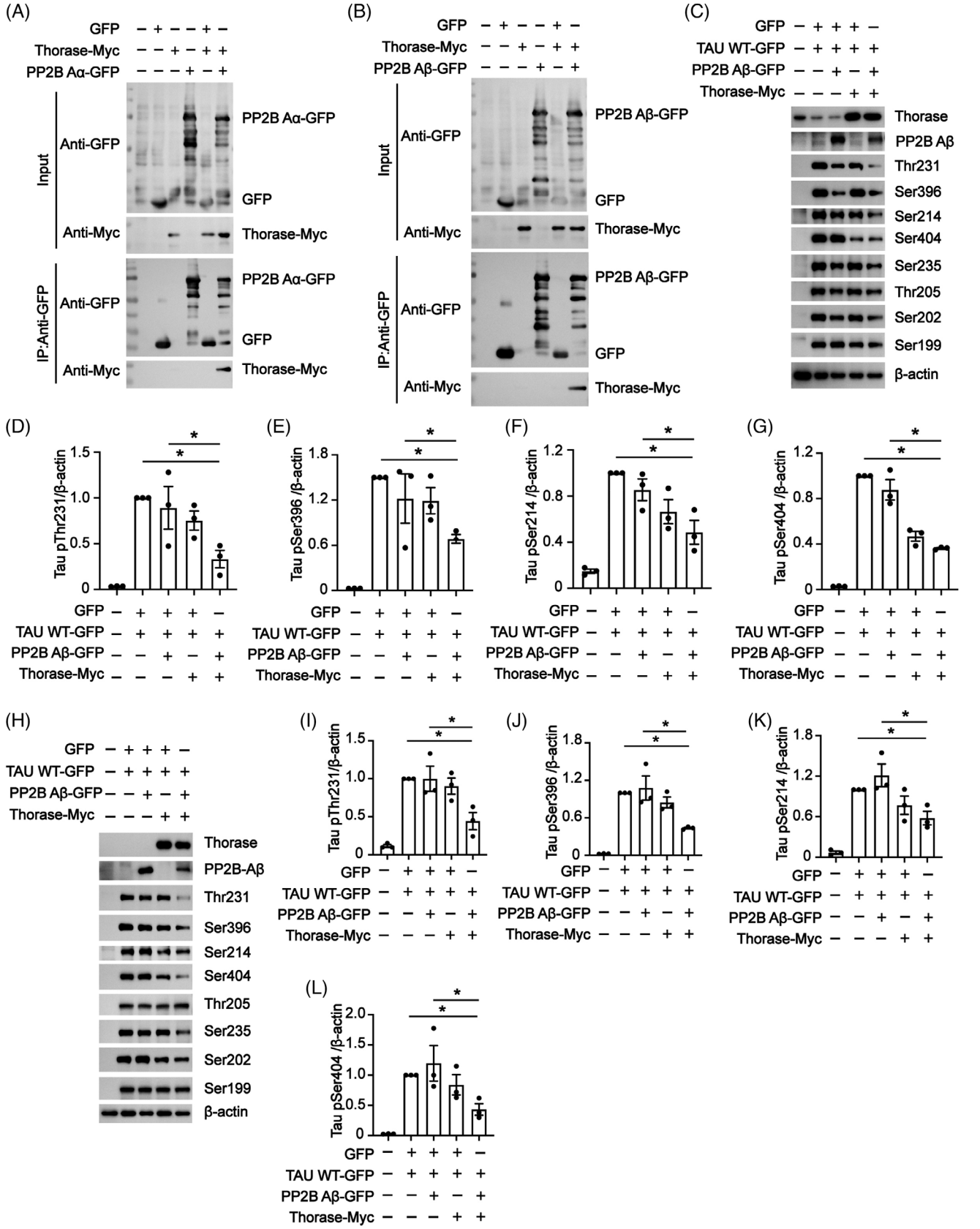

FIGURE 4 Thorase regulates the phosphorylation of the tau protein by targeting the phosphatase PP2B proteins. (A) Co-immunoprecipitation analysis of Thorase with PP2B Aα isomers using agarose GFP-trap Beads. (B) Co-immunoprecipitation analysis of Thorase with PP2B Aβ isomers using agarose GFP-trap Beads. (C) Western blot analysis of the phosphorylated tau protein levels at different sites when co-transfected

difference (Figure 3C,D). These results, taken together, suggest that Thorase regulates tau phosphorylation by targeting specific kinases or phosphatases.

3.5 | Thorase regulates the phosphorylation of the tau protein by targeting the phosphatase PP2B proteins

Next, we focused on determining whether Thorase interacts directly with phosphatase PP2B, a major phosphatase for the dephosphorylation of tau proteins. Thorase-Myc expressing plasmids were cotransfected with PP2B Aα-GFP or PP2B Aβ-GFP in HEK293T cells. Co-immunoprecipitation assay showed that Thorase interacted with both PP2B Aα and PP2B Aβ isomers (Figure 4A,B). To further verify whether the interaction of Thorase with PP2B A subunit regulates the phosphorylation of tau proteins, Thorase-Myc expressing plasmids were cotransfected with PP2B Aβ-GFP in HeLa Thorase KO cells and HeLa WT cells under conditions of tau protein overexpression. Western blot analysis showed that cotransfection of Thorase and PP2B-Aβ resulted in decreased levels of phosphorylated tau at Thr231, Ser396, Ser404, and Ser214 sites (Figure 4C–G); no significant differences were observed in the levels of tau phosphorylation at the Ser202, Ser235, Thr205, or Ser199 sites in the HeLa cells (Figure 4C and Figure S3A–D).

Similarly, in HeLa Thorase KO cells, we also found that cotransfection of Thorase and PP2B Aβ led to a decrease in the level of phosphorylated tau at Thr231, Ser396, Ser404, and Ser214 sites (Figure 4H–L). However, the levels of phosphorylated tau at the Ser235, Ser205, Ser202, and Ser199 sites showed no significant difference (Figure 4H and Figure S3E–H). In conclusion, these results validated that Thorase regulates tau protein phosphorylation through the interaction of Thorase with PP2B.

3.6 | Genetic deletion of Thorase in the brains results in enhanced Aβ deposition, astrocytosis, and activated microglia in an AD mouse model

The finding that Thorase regulates tau phosphorylation promoted us to determine whether Thorase also regulates Aβ pathology. Thorase cKO mice were crossed with the APP/PS1 (APP_{swe}/$PSEN1_{\Delta E9}$) transgenic (Tg) AD mouse model. In combination, Thorase cKO-APP/PS1 mice display high levels of human APP_{swe} and $PSEN1_{\Delta E9}$ and lack forebrain Thorase expression. Thorase cKO-APP/PS1 mice were born at Mendelian ratios and exhibited no gross anatomic defects or premature death. By 4 months of age, immunohistochemistry analysis of Aβ plaque burden using Aβ-specific monoclonal antibodies showed substantial plaques in Thorase cKO-APP/PS1 (Figure 5A,B). In contrast, no observable senile plaques were found in the forebrains of APP/PS1 mice. By using an Aβ *N*-terminal specific 6E10 monoclonal antibody, Western blot analysis showed significantly increased of Aβ levels in Thorase cKO-APP/PS1 mice (Figure 5C,D). Enzyme-linked immunosorbent assay (ELISA) quantitative analysis showed that Thorase deficiency significantly increased the levels of two major Aβ forms Aβ42 and $A\beta_{40}$ by greater than 3∼4 fold in the mouse brains of Thorase cKO-APP/PS1 mice compared with APP/PS1 mice (Figure 5E,F). Moreover, visualization of GFAP (Figure 5G,H) and Iba1 expression (Figure 5I,J) by immunohistochemistry revealed AD-like enhanced astrocytosis and activated microglia around the Aβ plaques in the forebrains of Thorase cKO-APP/PS1 mice. When Aβ plaque stimulates the microglia, these cells undergo a series of morphological changes that affect their morphology and function. Therefore, we further analyzed the morphology of microglia and discovered that the number of activated microglia increased in the cortex and hippocampus of Thorase cKO-APP/PS1 mice, whereas the number of resting microglia decreased (Figure 5K,L). Then we examined whether Thorase deficiency affected microglial phagocytosis to Aβ oligomers, the results of immunofluorescence staining showed that the content of Aβ was significantly decreased in the Thorase KO microglia cell, indicating that the phagocytotic activity to Aβ oligomers was significantly reduced in Thorase KO microglia compared with WT microglia (Figure 5M,N). Together, these results support a role for Thorase in regulating Aβ deposition and attenuation of disease pathogenesis in APP/PS1 mice.

3.7 | Thorase overexpression decreases Aβ deposition in AD model mice

For the same reason, we investigated the effects of Thorase overexpression on Aβ plaques in mouse brains. Immunohistochemical staining of Thorase cTg-APP/PS1 mouse brains revealed that the number of Aβ plaques decreased significantly in both the cortex and hippocampus (Figure 6A,B). Thioflavin-S staining also showed decreased Aβ plaques

Thorase-Myc plasmids with PP2B Aβ-GFP plasmids in HeLa cells with or without TAU WT-GFP plasmid transfection. (D) Quantification of the integral optical density (IOD) of phosphorylated tau at Thr231 site normalized to β-actin ($n = 3$) in panel C. (E) Quantification of the IOD of phosphorylated tau at Ser396 site normalized to β-actin ($n = 3$) in panel C. (F) Quantification of the IOD of phosphorylated tau at Ser214 site normalized to β-actin ($n = 3$) in panel C. (G) Quantification of the IOD of phosphorylated tau at Ser404 site normalized to β-actin ($n = 3$) in panel C. (H) Western blot analysis of the phosphorylated tau protein levels at different sites when co-transfected Thorase-Myc plasmids with PP2B Aβ-GFP plasmids in HeLa Thorase KO cells with or without Tay WT-GFP plasmid transfection. (I) Quantification of the IOD of phosphorylated tau at Thr231 site normalized to β-actin ($n = 3$) in panel H. (J) Quantification of the IOD of phosphorylated tau at Ser396 site normalized to β-actin ($n = 3$) in panel H. (K) Quantification of the IOD of phosphorylated tau at Ser214 site normalized to β-actin ($n = 3$) in panel H. (L) Quantification of the IOD of phosphorylated tau at Ser404 site normalized to β-actin ($n = 3$) in panel H. Data are presented as the mean ± standard error of measurement (SEM) determined using unpaired two-tailed Student's *t*-test. n.s., not significant; $^*p < 0.05$.

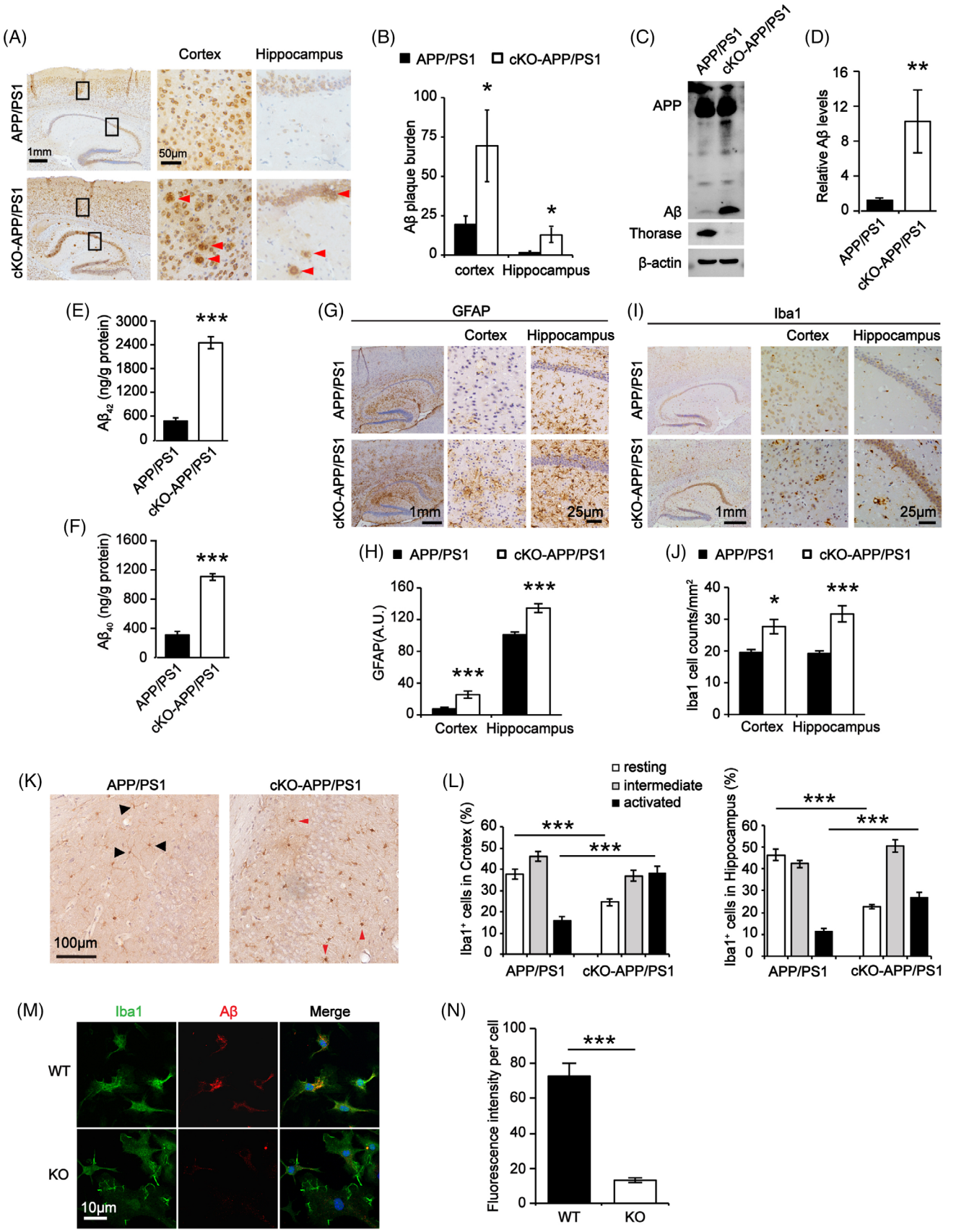

FIGURE 5 Genetic deletion of Thorase in the brains results in enhanced amyloid beta (Aβ) deposition, astrocytosis, and activated microglia in an AD mouse model. (A) Immunohistochemistry staining of Aβ plaque deposition in the cortex and hippocampus of Thorase cKO-APP/PS1 mice and APP/PS1 littermates ($n = 3$). The black rectangles represent the corresponding right images of high magnification in the cortex and

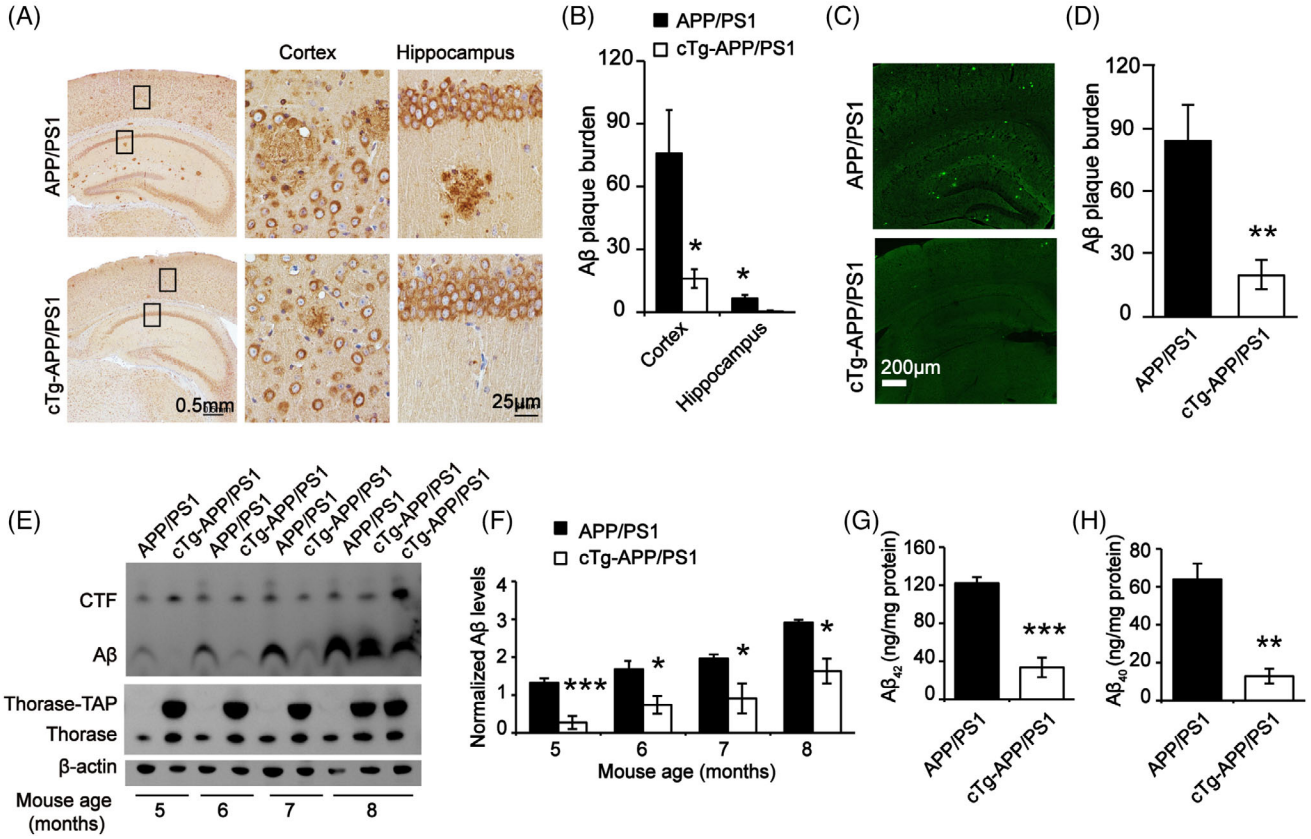

FIGURE 6 Thorase overexpression in the brain decreases amyloid beta (Aβ) deposition in Alzheimer's disease (AD) model mice. (A) Immunohistochemistry staining of Aβ plaque deposition in the cortex and hippocampus of Thorase cTg-APP/PS1 mice and APP/PS1 littermates ($n = 5$). The black rectangles represent the corresponding right images of high magnification in the cortex and hippocampus. Scale bar, 0.5 mm (left) and 25 μm (right). (B) Statistical analysis of Aβ plaque burden in the cortex and hippocampus of Thorase cTg-APP/PS1 mice, as shown in panel A. (C) Thioflavin-S staining of Aβ plaque deposition in the cortex from Thorase cTg-APP/PS1 mice and APP/PS1 littermates ($n = 5$). (D) Statistical analysis of Aβ plaque burden in the cortex of Thorase cTg-APP/PS1 mice, as shown in panel C. (E) Western blot analysis of Aβ from the forebrain tissue of Thorase cTg-APP/PS1 mice and APP/PS1 littermates at different months of age ($n = 3$). (F) Quantification of the integral optical density (IOD) of Aβ levels normalized to β-actin in panel E. (G) Enzyme-linked immunosorbent assay (ELISA) analysis of the content of Aβ42 proteins in the brain tissue from Thorase cTg-APP/PS1 mice and APP/PS1 littermates ($n = 4$). (H) ELISA analysis of the content of Aβ40 proteins in the brain tissue from Thorase cTg-APP/PS1 mice and APP/PS1 littermates ($n = 4$). Data are presented as the mean ± standard error of measurement (SEM) determined using unpaired two-tailed Student's *t*-test. n.s., not significant; $^{*}p < 0.05$, $^{**}p < 0.01$, and $^{***}p < 0.001$.

hippocampus. The red arrows indicate the Aβ plaques. Scale bar, 1 mm (left) and 50 μm (right). (B) Statistical analysis of Aβ plaque burden in the cortex and hippocampus of 4.5-month-old Thorase cKO-APP/PS1 mice, as shown in panel A. (C) Western blot analysis of Aβ from the forebrain tissue of Thorase cKO-APP/PS1 mice and APP/PS1 littermates at the age of 4.5 months ($n = 5$). (D) Quantification of the integral optical density (IOD) of Aβ levels normalized to β-actin in panel C. (E) Enzyme-linked immunosorbent assay (ELISA) analysis of the content of Aβ42 proteins in the brain tissue from Thorase cKO-APP/PS1 mice and APP/PS1 littermates ($n = 3$). (F) ELISA analysis of the content of Aβ40 proteins in the brain tissue from Thorase cKO-APP/PS1 mice and APP/PS1 littermates ($n = 3$). (G) Immunohistochemistry staining of GFAP in the cortex and hippocampus of 5-month-old Thorase cKO-APP/PS1 mice and APP/PS1 littermates ($n = 3$). Scale bar, 1 mm (left) and 25 μm (right). (H) Statistical analysis of GFAP in the cortex and hippocampus of Thorase cKO-APP/PS1 mice and APP/PS1 littermates, as shown in panel G. (I) Immunohistochemistry staining of Iba1 in the cortex and hippocampus of 5-month-old Thorase cKO-APP/PS1 mice and APP/PS1 littermates ($n = 3$). Scale bar, 1 mm (left) and 25 μm (right). (J) Statistical analysis of Iba1 in the cortex and hippocampus of Thorase cKO-APP/PS1 mice and APP/PS1 littermates, as shown in panel I. (K) Immunohistochemistry staining of Iba1 in the cortex and hippocampus of 5-month-old Thorase cKO-APP/PS1 mice and APP/PS1 littermates ($n = 3$). The black arrows indicate the resting microglia, whereas the red arrows indicate the fully activated microglia. Scale bar, 100 μm. (L) Statistical analysis of the percentage of microglia cells in three different states in the cortex and hippocampus of Thorase cKO-APP/PS1 mice and APP/PS1 littermates, as shown in panel K. (M) Immunofluorescence staining of Aβ plaque (red) and microglia (green) of Thorase KO and WT microglia cell ($n = 3$). Scale bar, 10 μm. (N) Statistical analysis of fluorescence intensity of Thorase KO and WT microglia cells as shown in panel M. Data are presented as the mean ± standard error of measurement (SEM) determined using unpaired two-tailed Student's *t*-test. n.s., not significant; $^{*}p < 0.05$, $^{**}p < 0.01$, and $^{***}p < 0.001$.

Alzheimer's & Dementia®
THE JOURNAL OF THE ALZHEIMER'S ASSOCIATION

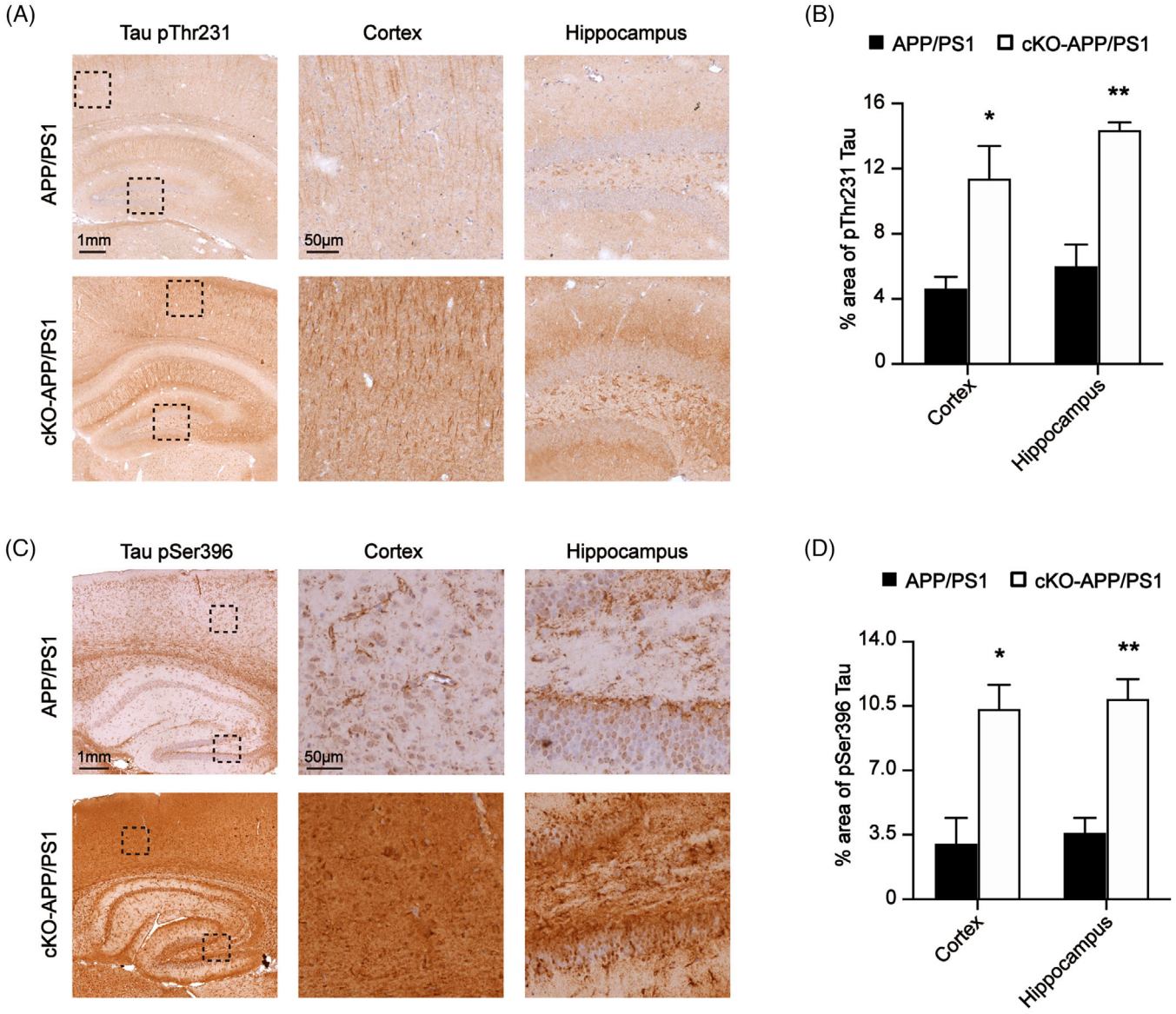

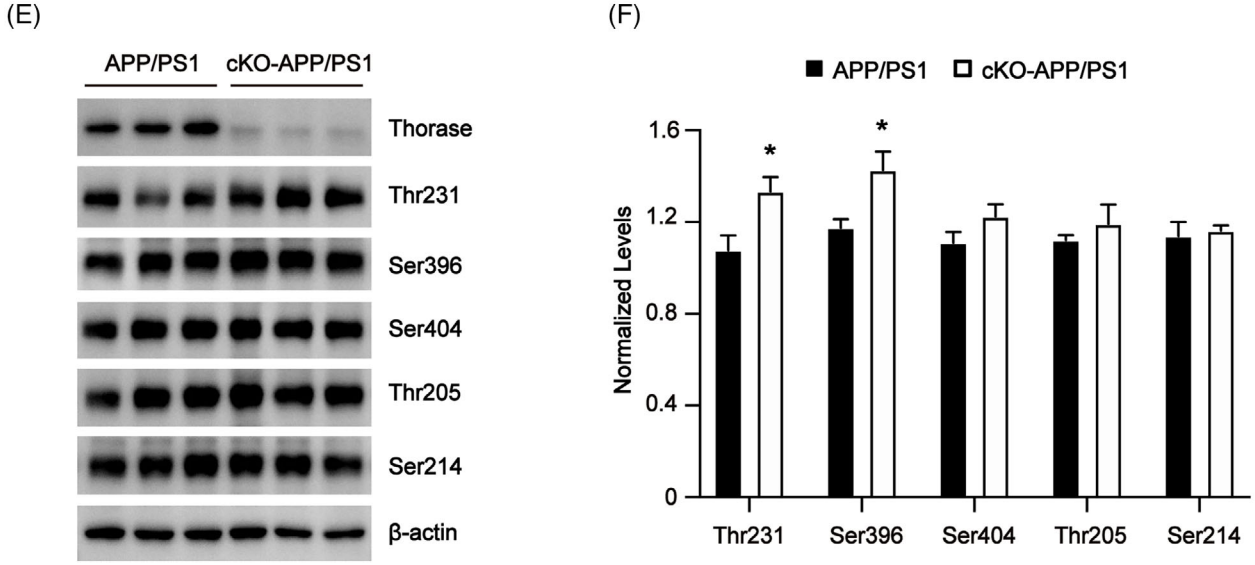

in Thorase cTg-APP/PS1 mouse brains (Figure 6C,D). Then we detected Aβ deposition in the brain tissue of mice at different ages. Western blot analysis of Thorase cTg-APP/PS1 mice and their APP/PS1 littermates showed that Aβ deposition increased with age, and compared to that in littermates of the same age, Aβ deposition decreased significantly in Thorase cTg-APP/PS1 mouse brains (Figure 6E,F). ELISA also revealed lower levels of both the Aβ42 and $A\beta_{40}$ proteins in Thorase cTg-APP/PS1 brain tissue (Figure 6G,H), consistent with previous findings. Overall, these findings suggest that Thorase overexpression reduces tau protein hyperphosphorylation and Aβ plaque deposition in the brains of mice, indicating the potential neuroprotective role of Thorase in AD.

3.8 | Thorase cKO-APP/PS1 mice exhibit increased levels of tau protein phosphorylation at Thr231 and Ser396 sites

Next, we sought to determine whether there are elevated levels of hyperphosphorylated tau proteins in Thorase cKO-APP/PS1 mice compared with their APP/PS1 littermates. Immunohistochemical analysis showed that Thorase cKO-APP/PS1 mice exhibited higher levels of hyperphosphorylated tau proteins at Thr231 (Figure 7A,B) and Ser396 (Figure 7C,D) sites than those in their APP/PS1 littermates. Western blot analysis also revealed increased levels of the tau protein phosphorylated at the Thr231 and Ser396 sites in the Thorase cKO-APP/PS1 mice (Figure 7E,F). These findings suggest collectively that Thorase regulates both the Aβ metabolism and the phosphorylation of tau protein, two major pathogeneses of AD.

3.9 | Thorase cKO-APP/PS1 mice exhibit enhanced neuroinflammation in the brain

Next, we examined the microglia and the neuroinflammation in the brains of Thorase cKO-APP/PS1 mice. Immunofluorescence staining showed that there were more microglia and apoptosis-associated speck-like protein containing a CARD (ASC) proteins around the Aβ plaques in the brains of Thorase cKO-APP/PS1 mice than those of their APP/PS1 littermates (Figure 8A,B). To determine the impact of Thorase deletion on inflammasome activation, we further examined the levels of inflammasome proteins in the brain tissues of Thorase cKO-APP/PS1 mice and their APP/PS1 littermates. Western blot analysis showed increased expression levels of the NLRP3, Pro Caspase-1, and ASC proteins in the brains of Thorase cKO-APP/PS1 mice (Figure 8C,D).

When the inflammasome is activated, pro-IL-1β is cleaved, which leads to the release of IL-1β. Therefore, we measured the levels of inflammatory factors in mouse brain tissues. ELISA showed that the levels of the inflammatory factors IL-1β and TNFα were elevated significantly in Thorase cKO-APP/PS1 mice (Figure 8E,F). Overall, Thorase cKO-APP/PS1 mice exhibited significantly increased levels of NLRP3 inflammasome activation and aggravated neuroinflammation.

3.10 | Elevated Aβ plaque deposition induces significantly increased inflammation via microglial dysfunction in Thorase cKO-APP/PS1 mice

Previous studies have shown that Aβ peptide deposition triggers a violent immune response in microglia and exacerbates the release of inflammatory cytokines.[2] Therefore, we isolated microglia from Thorase KO and WT mice and stimulated them with LPS, ATP, and Aβ peptides, respectively. Western blot analysis indicated that the intracellular assembly and activation of the NLRP3 inflammasomes were more pronounced upon stimulation with Aβ peptides in Thorase KO microglia (Figure 8G). In addition, the levels of Pro-GSDMD and Pro-Caspase 1 were found to be significantly elevated in Thorase KO microglia (Figure 8G). We subsequently measured lactate dehydrogenase (LDH) release by pyroptotic cells in the cell culture supernatant and found that LDH levels were significantly higher in Thorase KO microglia in the basal state than WT microglia (Figure 8H). Moreover, when cells were stimulated with an NLRP3 inflammasome activator, such as ATP or Aβ peptide, the pyroptosis ratio was increased significantly (Figure 8H). In addition, Thorase KO microglia were more significantly upregulated when stimulated with the NLRP3 inflammasome activator, and this phenomenon was more significant after long-term exposure to the Aβ peptide (Figure 8H).

We subsequently measured the levels of inflammatory factors released by microglia and found no significant difference in IL-1β release between WT and Thorase KO microglia when they were at rest. However, when stimulated with the inflammasome activator LPS or the Aβ peptide, Thorase KO microglia released significantly more IL-1β than WT microglia did (Figure 8I). The effect of the Aβ peptide on IL-1β release was significantly greater than that of ATP stimulation

FIGURE 7 Thorase cKO-APP/PS1 mice exhibit increased levels of tau protein phosphorylation at Thr231 and Ser396 sites. (A) Immunohistochemistry staining of phosphorylated tau protein at Thr231 sites in the cortex and hippocampus of 5-month-old Thorase cKO-APP/PS1 mice and APP/PS1 littermates ($n = 4$). Scale bar, 500 mm (left) and 100 μm (right). (B) Quantification of the % area of phosphorylated tau protein at Thr231 site in the cortex and hippocampus in panel A. (C) Immunohistochemistry staining of phosphorylated tau protein at Ser396 sites in the cortex and hippocampus of 5-month-old Thorase cKO-APP/PS1 mice and APP/PS1 littermates ($n = 3$). (D) Quantification of the % area of phosphorylated tau protein at Ser396 site in the cortex and hippocampus in panel C. (E) Western blot analysis of the levels of phosphorylated tau protein at several sites from the brain tissue of Thorase cKO-APP/PS1 mice and their APP/PS1 littermates at the age of 5 months ($n = 6$). (F) Quantification of the integral optical density (IOD) of phosphorylated tau protein at Thr231, Ser396, Ser404, Thr205, and Ser214 site normalized to β-actin in panel (E). Data are presented as the mean ± standard error of measurement (SEM) determined using unpaired two-tailed Student's *t*-test. n.s., not significant; $^*p < 0.05$.

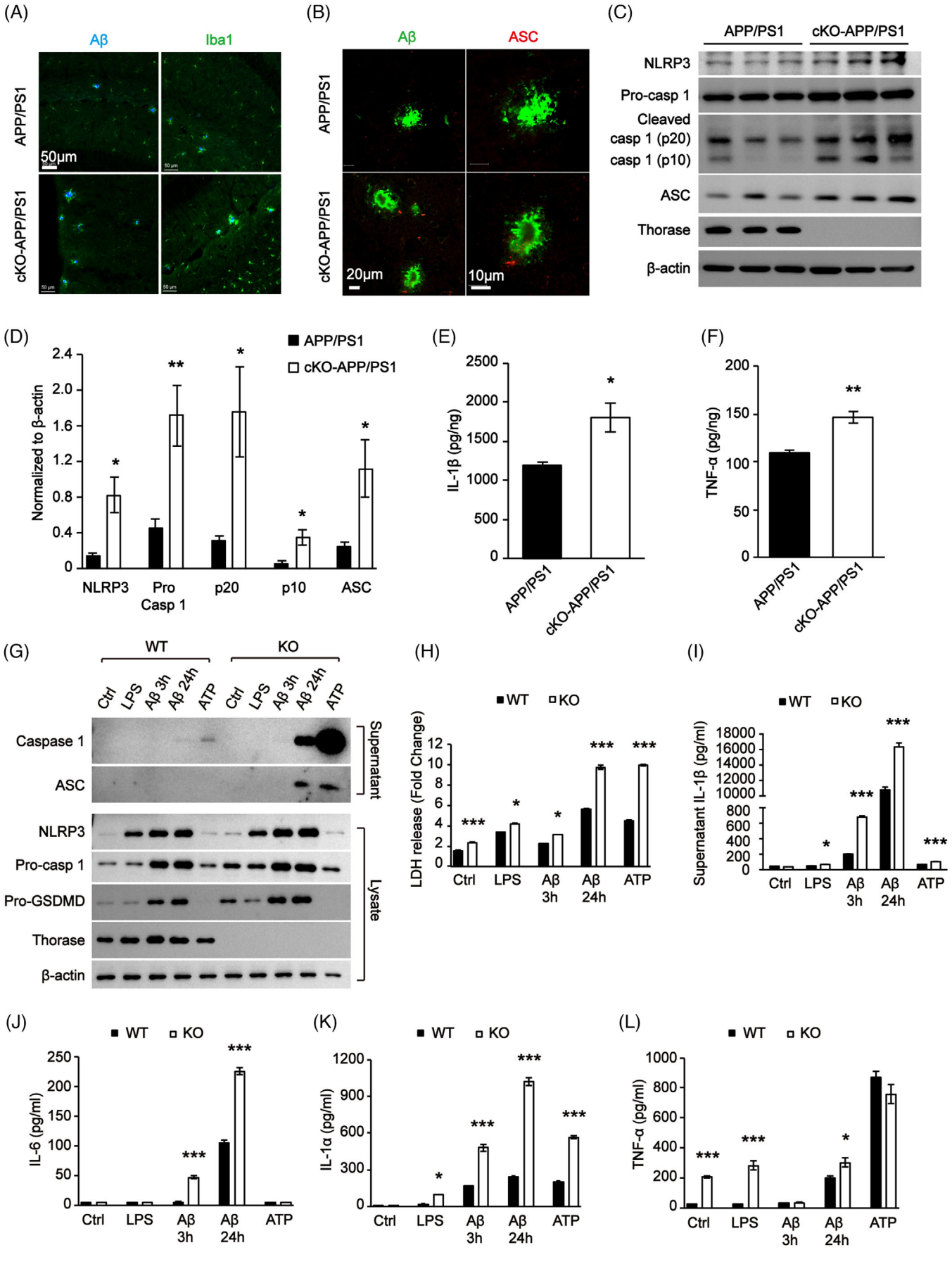
(A)
Aβ
Iba1
APP/PS1
cKO-APP/PS1
50μm
(B)
Aβ
ASC
APP/PS1
cKO-APP/PS1
20μm
10μm
(C)
APP/PS1
cKO-APP/PS1
NLRP3
Pro-casp 1
Cleaved casp 1 (p20)
casp 1 (p10)
ASC
Thorase
β-actin
(D)
APP/PS1
cKO-APP/PS1
Normalized to β-actin
NLRP3
Pro Casp 1
p20
p10
ASC
(E)
IL-1β (pg/ng)
APP/PS1
cKO-APP/PS1
(F)
TNF-α (pg/ng)
APP/PS1
cKO-APP/PS1
(G)
WT
KO
Ctrl
LPS
Aβ 3h
Aβ 24h
ATP
Caspase 1
ASC
Supernatant
NLRP3
Pro-casp 1
Pro-GSDMD
Thorase
β-actin
Lysate
(H)
WT
KO
LDH release (Fold Change)
Ctrl
LPS
Aβ 3h
Aβ 24h
ATP
(I)
WT
KO
Supernatant IL-1β (pg/ml)
Ctrl
LPS
Aβ 3h
Aβ 24h
ATP
(J)
WT
KO
IL-6 (pg/ml)
Ctrl
LPS
Aβ 3h
Aβ 24h
ATP
(K)
WT
KO
IL-1α (pg/ml)
Ctrl
LPS
Aβ 3h
Aβ 24h
ATP
(L)
WT
KO
TNF-α (pg/ml)
Ctrl
LPS
Aβ 3h
Aβ 24h
ATP

(Figure 8I). These results indicated that the deposition of Aβ plaques in brain tissue could induce intense inflammation in the nervous system and that long-term exposure to the Aβ peptides could significantly increase the release of IL-1β. These findings suggest that Thorase KO microglia are more sensitive to inflammatory stimulations.

Next we measured the levels of several other proinflammatory cytokines in the cell culture supernatant using ELISA kits. The results showed that the levels of IL-1α, IL-6, and TNFα were substantially higher in Thorase KO microglia when stimulated with Aβ peptides, but the changes in these inflammatory factors were not entirely due to NLRP3 inflammasome activation (Figure 8J–L).

4 | DISCUSSION

Alzheimer's disease is one of the most common neurodegenerative diseases and has two pathological hallmarks, the first being extracellular Aβ deposition in the cortex and hippocampus, which leads to senile plaques. The second hallmark is the accumulation of the intracellular hyperphosphorylated tau protein, which leads to NFTs and neuronal death,[33] along with the activation of microglia and astrocytes (severe neuroinflammation), mitochondrial dysfunction, and synapse loss (neurodegeneration).[34,35] Nonetheless, the exact pathogenesis and precise molecular changes in AD remain unclear. Furthermore, these main hallmarks interact with each other and accelerate the toxicity and spread of abnormal proteins to form aggregates in vivo, resulting in synergistic effects on the progression of AD.[36–38]

Thorase is an AAA^+ ATPase protein that is located on the mitochondrial outer membrane.[39] Thorase can induce conformational changes in several substrate proteins and provide ATP to facilitate a variety of cellular processes necessary for life, including cell cycle regulation, organelle assembly, protein degradation, DNA repair, and intracellular transport.[18] Our previous study found that Thorase cKO mice exhibited impaired cognitive function.[16] In this study we found a decrease of Thorase expression in brain tissues from patients with AD compared with age-matched donors without any symptoms of AD. We also found that Thorase deficiency resulted in tau protein hyperphosphorylation at Ser396, Thr231, Thr205, and Ser404 sites in Thorase cKO mice. Moreover, Thorase deletion in the forebrain led to significantly elevated Aβ plaque deposition and aggravated neuroinflammation, as indicated by an increased number of activated microglia in Thorase cKO-APP/PS1 mouse brains. Our previous studies found that Thorase provides protection against ischemic injury in vivo.[19] Here we also found that Thorase overexpression led to decreased Aβ plaque deposition in an AD mouse model and reduced tau protein hyperphosphorylation at Ser396, Thr231, and Ser404 sites in the brains of Thorase cTg mice, suggesting that Thorase may constitute a novel therapeutic strategy for treating and reducing pathology in AD.

Previous studies have shown that for the proper function of the tau protein, tau phosphorylation requires an equilibrium between protein kinases and phosphatases.[40,41] It is generally believed that a deficiency in brain phosphatase activity in patients with AD may be the main cause of abnormal hyperphosphorylation of the tau protein. Here we identified abnormal phosphorylation of tau protein at specific sites that were affected when Thorase was absent or overexpressed, as well as the expression levels and activities of protein kinases and protein phosphatases. Next we verified that Thorase interacts directly with the PP2B A subunit, a crucial phosphatase for tau dephosphorylation. As a result, Thorase deletion in the forebrain led to the aggregation of hyperphosphorylated tau protein in Thorase cKO mice.

As the resident innate immune cells of the central nervous system, microglia play a crucial role in regulating brain homeostasis and mediating immune responses in AD.[42] Recent studies have identified a broad range of microglial phenotypes in neurodegenerative disorders, from proinflammatory to neuroprotective effects, which makes it difficult to discern their role in different stages.[43,44] In this study we also found that activated microglia and astrocytes as well as the levels of the inflammasome proteins NLRP3, Pro-Caspase-1, and ASC increased in Thorase cKO-APP/PS1 mouse brains. Thorase deficiency resulted in elevated levels of IL-6, TNFα, and the IL-1α inflammasome when stimulated with Aβ. In addition, long-term exposure to Aβ peptides induced a significant increase in the pyroptosis ratio in Thorase KO microglia.

FIGURE 8 Elevated amyloid beta (Aβ) plaque deposition induces significantly increased inflammation via microglial dysfunction in Thorase cKO-APP/PS1 mice. (A) Immunofluorescence staining of Aβ plaque (blue) and microglia (green) in the cortex and hippocampus of Thorase cKO-APP/PS1 mice and APP/PS1 littermates ($n = 3$). Scale bar, 50 μm. (B) Immunofluorescence staining of Aβ plaque (green) and ASC (red) in the brain tissue of Thorase cKO-APP/PS1 mice and APP/PS1 littermates ($n = 3$). Scale bar, 20 μm (left) and 10 μm (right). (C) Western blot analysis of the levels of NLRP3 inflammasome-related protein from the forebrain tissue of Thorase cKO-APP/PS1 mice and APP/PS1 littermates ($n = 3$). (D) Quantification of the integral optical density (IOD) of the levels of NLRP3 inflammasome-related protein normalized to β-actin in panel C. (E) Enzyme-linked immunosorbent assay (ELISA) analysis of interleukin (IL)-1β inflammatory cytokines levels in the brain tissue from Thorase cKO-APP/PS1 mice and APP/PS1 littermates ($n = 3$). (F) ELISA analysis of tumor necrosis factor α (TNFα) inflammatory cytokines levels in the brain tissue from Thorase cKO-APP/PS1 mice and APP/PS1 littermates ($n = 3$). (G) Western blot analysis of the levels of NLRP3 inflammasome-related protein under different activations in Thorase KO and WT microglia cell lysate and supernatant ($n = 3$). (H) LDH released assay in the supernatant of Thorase KO and WT microglia cells under different stimulated conditions. (I) ELISA analysis of the levels of IL-1β inflammatory cytokines in the supernatant of Thorase KO and WT microglia cells under different stimulated conditions. (J) ELISA analysis of the levels of IL-6 inflammatory cytokines in the supernatant of Thorase KO and WT microglia cells under different stimulated conditions. (K) ELISA analysis of the levels of IL-1α inflammatory cytokines in the supernatant of Thorase KO and WT microglia cells under different stimulated conditions. (L) ELISA analysis of the levels of TNFα inflammatory cytokines in the supernatant of Thorase KO and WT microglia cells under different stimulated conditions. Data are presented as the mean ± standard error of measurement (SEM) determined using unpaired two-tailed Student's *t*-test. n.s., not significant; $^*p < 0.05$ and $^{**}p < 0.01$.

Thorase deletion also impaired microglial phagocytosis of Aβ. Previous studies demonstrated that microglia and NLRP3 inflammasome activation could induce tau hyperphosphorylation and Aβ aggregation and high level of tau phosphorylation could also activate the NLRP3 inflammasome and IL-1β release.[13,14] In addition, the elevated Aβ deposition may also be due to the dysfunctional autophagy in Thorase KO mice, which needs to be further investigated in future studies. These findings indicate that Thorase deficiency exacerbates Aβ pathology and tau protein phosphorylation, thereby worsening a vicious cycle within the pathological process of AD.

In summary, our findings demonstrate that Thorase represents a promising therapeutic target in AD, as it plays a crucial role in both Aβ plaque deposition and the phosphorylation of the tau protein in vivo through distinct mechanisms.

AUTHOR CONTRIBUTIONS

Conceptualization: Jianmin Zhang, Wei He, Jia Yang, Hui Chen, Fei Gao, and Han Zhang. *Methodology*: Jia Yang, Menghua Cai, Fei Gao, and Han Zhang. *Investigation*: Jia Yang, Menghua Cai, Fei Gao, Han Zhang, Chao Li, Jingyi Han, Yue Wang, and Yi Xu. *Validation*: Menghua Cai, Jia Yang, Yi Xu, and Fei Gao. *Writing – original draft preparation*: Jianmin Zhang, Jia Yang, Menghua Cai, Han Zhang, and Fei Gao. *Writing – review and editing*: Hui Chen, Wei He, and Jianmin Zhang. *Resources*: Yu Hu and Hui Chen. *Supervision*: Hui Chen, Jianmin Zhang, and Wei He. *Funding acquisition*: Yi Xu, Hui Chen, Jianmin Zhang, and Wei He. All authors have read and agreed to the published version of the manuscript.

ACKNOWLEDGMENTS

This research was supported by the National Key Research and Development Program of China (2022YFC3602004), the CAMS Initiative for Innovative Medicine (2021-I2M-1-005, 2021-I2M-1-035, and 2021-I2M-1-053), and the National Natural Science Foundation of China (U20A20374, 32270915, 82071791). This study was also supported by the Institute of Basic Medical Sciences, Chinese Academy of Medical Sciences, Neuroscience Center, and the China Human Brain Banking Consortium.

CONFLICT OF INTEREST STATEMENT

The authors declare no conflicts of interest. Author disclosures are available in the supporting information.

CONSENT STATEMENT

All procedures in this study were conducted in accordance with the Ethics Committee of the Institute of Basic Medical Sciences-Chinese Academy of Medical Sciences (CAMS) approved protocols (Approval Number: 2022YFC3602004). All AD and non-AD human samples were provided by National Human Brain Bank for Development and Function, Chinese Academy of Medical Sciences and Peking Union Medical College, Beijing, China. All donors provided informed consent for using their donated body tissue for medical research.

ORCID

Jianmin Zhang https://orcid.org/0000-0003-4765-0812

REFERENCES

1. Lee S, Cho HJ, Ryu JH. Innate immunity and cell death in Alzheimer's disease. *ASN Neuro*. 2021;13:17590914211051908. doi:10.1177/17590914211051908
2. Heneka MT, Carson MJ, El Khoury J, et al. Neuroinflammation in Alzheimer's disease. *Lancet Neurol*. 2015;14(4):388-405. doi:10.1016/S1474-4422(15)70016-5
3. Chen GF, Xu TH, Yan Y, et al. Amyloid beta: structure, biology and structure-based therapeutic development. *Acta Pharmacol Sin*. 2017;38(9):1205-1235. doi:10.1038/aps.2017.28
4. He Z, Guo JL, McBride JD, et al. Amyloid-β plaques enhance Alzheimer's brain tau-seeded pathologies by facilitating neuritic plaque tau aggregation. *Nat Med*. 2018;24(1):29-38. doi:10.1038/nm.4443
5. Selkoe DJ, Hardy J. The amyloid hypothesis of Alzheimer's disease at 25 years. *EMBO Mol Med*. 2016;8(6):595-608. doi:10.15252/emmm.201606210
6. Chong FP, Ng KY, Koh RY, Chye SM. Tau proteins and tauopathies in Alzheimer's disease. *Cell Mol Neurobiol*. 2018;38(5):965-980. doi:10.1007/s10571-017-0574-1
7. Sinsky J, Pichlerova K, Hanes J. Tau protein interaction partners and their roles in Alzheimer's disease and other tauopathies. *Int J Mol Sci*. 2021;22(17):9207. doi:10.3390/ijms22179207
8. Wang JZ, Grundke-Iqbal I, Iqbal K. Kinases and phosphatases and tau sites involved in Alzheimer neurofibrillary degeneration. *Eur J Neurosci*. 2007;25(1):59-68. doi:10.1111/j.1460-9568.2006.05226.x
9. Torres AK, Rivera BI, Polanco CM, Jara C, Tapia-Rojas C. Phosphorylated tau as a toxic agent in synaptic mitochondria: implications in aging and Alzheimer's disease. *Neural Regen Res*. 2022;17(8):1645-1651. doi:10.4103/1673-5374.332125
10. Wang JZ, Xia YY, Grundke-Iqbal I, Iqbal K. Abnormal hyperphosphorylation of tau: sites, regulation, and molecular mechanism of neurofibrillary degeneration. *J Alzheimers Dis*. 2013;33(Suppl 1):S123-139. doi:10.3233/JAD-2012-129031
11. Götz J, Xia D, Leinenga G, Chew YL, Nicholas H. What renders TAU toxic. *Front Neurol*. 2013;4:72. doi:10.3389/fneur.2013.00072
12. Hansen DV, Hanson JE, Sheng M. Microglia in Alzheimer's disease. *J Cell Biol*. 2018;217(2):459-472. doi:10.1083/jcb.201709069
13. Zhang Y, Dong Z, Song W. NLRP3 inflammasome as a novel therapeutic target for Alzheimer's disease. *Signal Transduct Target Ther*. 2020;5(1):37. doi:10.1038/s41392-020-0145-7
14. Ising C, Venegas C, Zhang S, et al. NLRP3 inflammasome activation drives tau pathology. *Nature*. 2019;575(7784):669-673. doi:10.1038/s41586-019-1769-z
15. Heneka MT, Kummer MP, Stutz A, et al. NLRP3 is activated in Alzheimer's disease and contributes to pathology in APP/PS1 mice. *Nature*. 2013;493(7434):674-678. doi:10.1038/nature11729
16. Zhang J, Wang Y, Chi Z, et al. The AAA+ ATPase Thorase regulates AMPA receptor-dependent synaptic plasticity and behavior. *Cell*. 2011;145(2):284-299. doi:10.1016/j.cell.2011.03.016
17. Chen YC, Umanah GKE, Dephoure N, et al. Msp1/ATAD1 maintains mitochondrial function by facilitating the degradation of mislocalized tail-anchored proteins. *EMBO J*. 2014;33(14):1548-1564. doi:10.15252/embj.201487943
18. Wang L, Walter P. Msp1/ATAD1 in protein quality control and regulation of synaptic activities. *Annu Rev Cell Dev Biol*. 2020;36:141-164. doi:10.1146/annurev-cellbio-031220-015840
19. Zhang J, Yang J, Wang H, et al. The AAA + ATPase Thorase is neuroprotective against ischemic injury. *J Cereb Blood Flow Metab*. 2019;39(9):1836-1848. doi:10.1177/0271678X18769770
20. Yao F, Zhang K, Zhang Y, et al. Identification of blood biomarkers for Alzheimer's disease through computational prediction and experimental validation. *Front Neurol*. 2018;9:1158. doi:10.3389/fneur.2018.01158

21. Brody AH, Nies SH, Guan F, et al. Alzheimer risk gene product Pyk2 suppresses tau phosphorylation and phenotypic effects of tauopathy. *Mol Neurodegener*. 2022;17(1):32. doi:10.1186/s13024-022-00526-y
22. Li L, Zheng J, Wu X, Jiang H. Mitochondrial AAA-ATPase Msp1 detects mislocalized tail-anchored proteins through a dual-recognition mechanism. *EMBO Rep*. 2019;20(4):e46989. doi:10.15252/embr.201846989
23. Casanova E, Fehsenfeld S, Mantamadiotis T, et al. A CamKIIalpha iCre BAC allows brain-specific gene inactivation. *Genesis*. 2001;31(1):37-42. doi:10.1002/gene.1078
24. Limaye A, Cho K, Hall B, Khillan JS, Kulkarni AB. Genotyping protocols for genetically engineered mice. *Curr Protoc*. 2023;3(11):e929. doi:10.1002/cpz1.929
25. Saura J, Tusell JM, Serratosa J. High-yield isolation of murine microglia by mild trypsinization. *Glia*. 2003;44(3):183-189. doi:10.1002/glia.10274
26. Shi SR, Key ME, Kalra KL. Antigen retrieval in formalin-fixed, paraffin-embedded tissues: an enhancement method for immunohistochemical staining based on microwave oven heating of tissue sections. *J Histochem Cytochem*. 1991;39(6):741-748. doi:10.1177/39.6.1709656
27. Donaldson JG. Immunofluorescence staining. *Curr Protoc Cell Biol*. 2001;Chapter 4:Unit 4.3. doi:10.1002/0471143030.cb0403s00
28. Guntern R, Bouras C, Hof PR, Vallet PG. An improved thioflavine S method for staining neurofibrillary tangles and senile plaques in Alzheimer's disease. *Experientia*. 1992;48(1):8-10. doi:10.1007/BF01923594
29. Lin JS, Ali J, Lai EM. Protein-protein interactions: co-immunoprecipitation. *Methods Mol Biol*. 2024;2715:273-283. doi:10.1007/978-1-0716-3445-5_18
30. Kohl TO, Ascoli CA. Direct competitive enzyme-linked immunosorbent assay (ELISA). *Cold Spring Harb Protoc*. 2017;2017(7):pdb.prot093740. doi:10.1101/pdb.prot093740
31. Kabakov AE, Gabai VL. Cell death and survival assays. *Methods Mol Biol*. 2018;1709:107-127. doi:10.1007/978-1-4939-7477-1_9
32. Gao F, Zhang H, Yang J, et al. ATPase thorase deficiency causes α-synucleinopathy and Parkinson's disease-like behavior. *Cells*. 2022;11(19):2990. doi:10.3390/cells11192990
33. Castillo-Carranza DL, Guerrero-Muñoz MJ, Kayed R. Immunotherapy for the treatment of Alzheimer's disease: amyloid-β or tau, which is the right target? *Immunotargets Ther*. 2014;3:19-28. doi:10.2147/ITT.S40131
34. Heppner FL, Ransohoff RM, Becher B. Immune attack: the role of inflammation in Alzheimer disease. *Nat Rev Neurosci*. 2015;16(6):358-372. doi:10.1038/nrn3880
35. Swerdlow RH, Burns JM, Khan SM. The Alzheimer's disease mitochondrial cascade hypothesis: progress and perspectives. *Biochim Biophys Acta*. 2014;1842(8):1219-1231. doi:10.1016/j.bbadis.2013.09.010
36. Ittner LM, Götz J. Amyloid-β and tau – a toxic pas de deux in Alzheimer's disease. *Nat Rev Neurosci*. 2011;12(2):65-72. doi:10.1038/nrn2967
37. Chabrier MA, Blurton-Jones M, Agazaryan AA, Nerhus JL, Martinez-Coria H, LaFerla FM. Soluble aβ promotes wild-type tau pathology in vivo. *J Neurosci*. 2012;32(48):17345-17350. doi:10.1523/JNEUROSCI.0172-12.2012
38. Ittner LM, Ke YD, Delerue F, et al. Dendritic function of tau mediates amyloid-beta toxicity in Alzheimer's disease mouse models. *Cell*. 2010;142(3):387-397. doi:10.1016/j.cell.2010.06.036
39. Fresenius HL, Wohlever ML. Sorting out how Msp1 maintains mitochondrial membrane proteostasis. *Mitochondrion*. 2019;49:128-134. doi:10.1016/j.mito.2019.07.011
40. Wang Y, Mandelkow E. Tau in physiology and pathology. *Nat Rev Neurosci*. 2016;17(1):5-21. doi:10.1038/nrn.2015.1
41. Yu CC, Jiang T, Yang AF, Du YJ, Wu M, Kong LH. Epigenetic modulation on tau phosphorylation in Alzheimer's disease. *Neural Plast*. 2019;2019:6856327. doi:10.1155/2019/6856327
42. Hemonnot AL, Hua J, Ulmann L, Hirbec H. Microglia in Alzheimer disease: well-known targets and new opportunities. *Front Aging Neurosci*. 2019;11:233. doi:10.3389/fnagi.2019.00233
43. Xu YJ, Au NPB, Ma CHE. Functional and phenotypic diversity of microglia: implication for microglia-based therapies for Alzheimer's disease. *Front Aging Neurosci*. 2022;14:896852. doi:10.3389/fnagi.2022.896852
44. Sobue A, Komine O, Yamanaka K. Neuroinflammation in Alzheimer's disease: microglial signature and their relevance to disease. *Inflamm Regen*. 2023;43(1):26. doi:10.1186/s41232-023-00277-3

SUPPORTING INFORMATION

Additional supporting information can be found online in the Supporting Information section at the end of this article.

How to cite this article: Zhang H, Cai M, Gao F, et al. Thorase deficiency causes both Aβ accumulation and tau hyperphosphorylation in mouse brain. *Alzheimer's Dement*. 2024;20:8769–8786. https://doi.org/10.1002/alz.14329